

Creep Life Forecasting of Weldment

J. Jelwan*, M. Chowdhry, G. Pearce

Department of Mechanical Engineering and Manufacturing, University of New South Wales, Sydney, Australia ,NSW 2052

Received 16 February 2011; accepted 2 March 2011

ABSTRACT

One of the yet unresolved engineering problems is forecasting the creep lives of weldment in a pragmatic way with sufficient accuracy. There are number of obstacles to circumvent including: complex material behavior, lack of accurate knowledge about the creep material behavior specially about the heat affected zones (HAZ), accurate and multi-axial creep damage models, etc. In general, creep life forecasting may be categorized into two groups, viz., those that are based on microscopic modeling and others that are based on macroscopic (phenomenological) concepts. Many different micro-structural processes may cause creep damage. The micro-structural processes highlight the fact that the creep damages can be due to cavity nucleation and growth. Dislocation creep is another mechanism with micro-structural features such as sub-grain formation and growth, new phase formation, such as the Z phase, coarsening leading to the dissolution of the MX phase. This leads to the removal of pinning precipitates, which allow local heterogeneous sub-grain growth, weakening due to this growth and also to the dissolution of the MX. These features normally lead to the earlier formation of tertiary creep and reduced life. Considering welded joints, the development of models for practical yet sufficiently accurate creep life forecasting based on micro-structural modeling becomes even more complicated due to variation of material in the base, weld and heat-affected-zone (HAZ) and variation of the micro-structure within HAZ and their interactions. So far, and until this date, none of the micro-structural models can forecast the creep life of industrial components with sufficient accuracy in an economic manner. There are several macroscopic (phenomenological) models for creep life forecasting, including: time-fraction rule, strain-fraction rule, the reference stress and skeletal stress method, continuum damage model, etc. Each of which has their own limitations. This paper gauges to a multi-axial yet pragmatic and simple model for creep life forecasting weldment operating at high temperature and subjected to an elastic-plastic-creep deformation.

© 2011 IAU, Arak Branch. All rights reserved.

Keywords: Strain energy density; Finite element Analysis; Creep; Weld; Stress/Strain analysis; Failure prediction.

1 INTRODUCTION

ENERGY is a primary input of any industrial operation. Energy is also a major input in sectors such as commerce, transport, and telecommunication etc. besides the wide range of services required in the household and industrial sectors. The initial source of energy comes from fossil fuels such as coal, oil and natural gases which play an important role in the development of technology and which cannot be underestimated for a tremendous and modern civilization for many years forefront. With this dependency, come large requirements for the reliable operation of the plant to constantly supply power, maximize its efficiency while at the same time operates in a safe environment. Such power plants contain some components which operate in creep range, where the welding is widely used for fabrication of structures such as pressure vessels. Due to the nature of this process, heat is applied into the material during welding. After cooling, as a result, microstructure and mechanical properties can be altered.

* Corresponding author. Tel.: +61 2 93856006; Fax: +61 2 9663 1222.

E-mail address: jad.jelwan@unsw.edu.au (J. Jelwan).

A critical area known as heat-affected-zone (HAZ) is formed after welding, which is generally an area of the welded structure that is prone to metallurgical problems during severe operating conditions where failure can endanger human life. Therefore, creep must be considered in integrity assessment and design of any industrial component that operates above $0.3 T_M$.

Predicting the remaining operating life of weld is a problem faced by many metallurgist and researcher. This is due to complicated service environments and stress conditions subjected on the structure elements of these vessels. The presence of weld imperfections such as slag inclusions at welds toes, undercut, lack of penetration, misalignment, etc., and effectively also reduces the life of the structures. Furthermore, welded structures experience complicated behavior due to the applied pressure and axial/biaxial load. In addition, the weld life is affected by the residual stress developed during the welding process.

Another characteristic for the failure of weld can be described by Le Chatelier Rule. In [1], Le Chatelier study the response of the structural elements of a material and explained the physical processes can cause plastic flow deformation arising from the mismatch interaction of the material properties caused by the external applied forces, which leads to a creep dislocation. The formation of an ordered dislocation structure is just an evolution process which tries to act against applied stresses. The point is that the high temperature conditions give the possibility of supplying the dislocation re-arrangement with energy which results in the substructure formation [2]. Many studies have been conducted on creep dislocation and many conclusions have been reported in the literature. For instance, new phase formation such as the Z phase has been investigated. The Z phase is defined as a coarsening leading to the dissolution of the MX phase. This phenomenon articulates to the removal of pinning precipitates, which allow local heterogeneous sub-grain growth, weakening due to this growth and also to the dissolution of the MX. These features normally lead to the earlier formation of tertiary creep and reduced life. However, the Z phase is not fully understood [2]. Also, it is difficult to moderate a consistent and logical assessment for the various kinetic dislocations observed. It is not clear whether Z phase actually forms from MX precipitates or directly with the absence of sub-grain. These observations may be acquiescent if it could be proved significantly different from the multi-material component such as a welded pipe for each of the PM, HAZ and WM.

Another available option to reduce the risks of failure, is the practice codes [3, 4]. For instance, the Code Case N-47 was the first high temperature design code published in 1987 which took into account the weakening effect of weldments by introducing reduction factors to make some allowance for poorer performance of welded joints, by assuming the weld to be a defect free structure. Similarly, the French Code RCC-MR and the British Energy practice code R5 have incorporated the same concepts. However, deficiencies are available in these current high temperature design codes where the life assessment procedure is expected to be too conservative. Also, the lack of experimental material properties data for each of the base material, heat-affected zone and weld material deviate the design quality to unfavorable result which can affect the power plant economically.

Consider a loaded welded vessel operating at high temperature in which the parent material (PM), heat affected zone (HAZ) and weld material (WM), each creep at different rates under a stress field which continues to deform even if the load is maintain constant, generating complex shear stress fields at the interface of these materials. The main reason for the deformation mechanism is that at high temperature, the grain boundary start to slide inducing stress concentration caused by the shear stress within the transitional zone between the HAZ and PM (or between the HAZ and WM). This coupled with uncertainty associated with creep material data especially those of HAZ, where creep manifests itself as gradual distortion. It is worth noting that creep cracks are formed, if the deformation of the inside grain cannot accommodate the shear deformation at grain boundaries and thus creep rupture of the welded joints is caused by a higher multi-axial stress/strain fields in short term creep rupture. Complexity of the problem would increase if there is additional plastic deformation when the welded joint is loaded due to rapid change of geometry at the joint with no volume change. Large amount of strain energy density is dissipated by this process. Energy absorption by plastic deformation (plastic strain energy density) is approximately computed to be greater by several orders of magnitude than through of the creep strain energy density. The appearance of the damaged regions is due to both the occurrence of plastic flow deformation on the fractured zone and the accumulation of creep strains within that critical zone.

There are several macroscopic (phenomenological) models for creep life forecasting, including: time-fraction rule, strain-fraction rule, the reference stress and skeletal stress method, continuum damage model, etc. Each of which has their own limitations. In order to improve the present situation, the very complex behavior of high temperature weldments has to be further understood. Recently, Zarrabi and Jelwan [5, 6] have proposed a relatively accurate model for life prediction of components that are subjected to an elastic-plastic-creep deformation. The model is based on the exhaustion of the strain energy density at the critical regions in the components such as the welded joints. This paper gauges to a multi-axial yet pragmatic and simple model for creep life forecasting weldments operating at high temperature for which the experimental results are available.

2 CREEP LIFE ASSESSMENT METHODS

Currently, a large amount of equipment in industry contains metallic components which must be designed and constructed or their lives extended to operate at high temperatures. The safety of these components and their economic operations will depend on how efficiently we can predict their creep lives. Creep life assessments using experimental approaches are usually time-consuming, expensive and not practical for routine industrial applications. Creep life assessments using analytical and numerical methods is also time consuming, expensive and beyond the usual engineering tasks. Also, the results obtained from these methods are not accurate because of the uncertainty involved with material data, loading conditions and constitutive equations. Therefore, there is a need for relatively simple life assessments methods that provide reasonable and conservative results on the bases of the less than ideal input data. In the industry, the most used method for life prediction is Robinson's linear fracture rule [7]. The life-fraction is defined by:

a) The time fraction rule:

$$\sum \frac{\Delta t_i(\sigma_{r_i})}{t_{r_i}(\sigma_{r_i})} = 1 \quad (1)$$

b) The strain fraction rule:

$$\sum \frac{\Delta \varepsilon_i(\sigma_{r_i})}{\varepsilon_{r_i}(\sigma_{r_i})} = 1 \quad (2)$$

or a mixture of the two [8]. However, Robinson rule does not couple the gradual degradation of the material with other constitutive properties. This can lead to large errors when analyzing a hyperstatic structure. If, for instance, the applied load on a hyperstatic structure is kept constant, the degradation leads to a redistribution of the stress with time. This means that an uninformed application of a design rule according to Eq. (2) gives an overly conservative estimate of the failure time[9]. In the case of multi-axially loaded components, experimental observations have shown the rupture stress (σ_r) depends on the effective stress, (σ_e), causing dislocation glide or grain boundary sliding and the maximum principal stress (σ_1) causing creep cavitations and usually this is taken to be a linear dependency of the form [10]:

$$\sigma_r = (1 - \alpha) + \alpha \sigma_e \quad (3)$$

where α a material parameter that depends on temperature. Eq. (3) is used to calculate the rupture stress at the skeletal point that is a point in the material where stress components are assumed to be time-invariant. Combining σ_r with the uniaxial creep rupture data will results in creep life of the component. The main shortcoming with this approach is that α is not known and its evaluation requires expensive creep testing of the component and it is time consuming and usually impractical. In practice, the analyst either assumes $\alpha = 1$ resulting in $\sigma_r = \sigma_e$ or $\alpha = 0$ resulting $\sigma_r = \sigma_1$ which adds to the analysis an inaccuracy of the predicted creep life. Another creep life prediction is based on the reference stress (σ_{ref}) method which also, assumes that there exists a time invariant stress when it is combined with uniaxial creep rupture data result in the creep life of the component. However, the reference stress method, in general, is a function of the effective and hydrostatic stresses but in practice this approach estimates using the effective stress only. Also, σ_{ref} is usually computed using the limit load P_L of the component where:

$$\sigma_{ref} = \frac{P \sigma_y}{P_L} \quad (4)$$

However, Eq. (4) is derived based on the lower bound theorem and underestimates the true σ_{ref} and therefore it could result in non-conservative life predictions. A potential function of the form defined by von Mises is used to obtain a reference stress (S) for the tube and which is given as [11, 12]:

$$S = K \frac{\sqrt{3}}{2} \frac{P_e}{\ln\left(\frac{d+H}{d-H}\right)} \tag{5}$$

where d and H are the tube mean diameter and thickness at any time t and K is a constant that depends on the geometry of the tube area which is being thinned and it is usually assumed to be equal to 1. However, this conservative assumption is thought to have some practical aspects embedded in it because , in practice ,it is usually difficult to determine the geometry of the pits precisely[12].Other methods for creep life predictions are based on : continuum damage mechanics (CDM) or microstructural models or direct creep measurements [13]. The empirical CDM has its origins in the attempts by Kachanov [14] and Rabotnov [15] in the 1950s to quantify the tertiary stage of creep, taking into account the redistribution of stresses and strains due to internal damage. A readable account of their work is given by Penny and Marriott [16]. Creep damage manifests itself as an accelerating (tertiary) rate in standard constant load tests and as a progressively decreasing stress in constant strain rate tests. The damage parameter w was introduced, the value of which is equal to zero for no damage and one for rupture or failure. The damage parameter was not meant to be measurable or definable property even though it was to represent the internal cavitations and rupture of the material. The effect of the damage parameter on stress is to magnify it by the factor $1/(1-w)$ due to a loss in load bearing cross section. Thus, the stress strain relation becomes:

$$\dot{\epsilon} = B \left(\frac{\sigma}{\sigma_0(1-w)} \right)^n \tag{6}$$

where the rate of change increase, \dot{w} is:

$$\dot{w} = G \left(\frac{\sigma}{(1-w)} \right)^m \tag{7}$$

And G and m are constants that can be determined by the experimental creep rupture data. The two equations can be solved simultaneously to give the remaining life fraction, RLF , as a function of w [17, 18]:

$$RLF = \left(1 - \frac{t}{t_r} \right) = (1-w)^{\frac{n\lambda}{\lambda-1}} \tag{8}$$

with

$$\lambda = \frac{e_r}{e} \tag{9}$$

where e and e_r are the strain at time t and the strain at rupture, respectively. This arrangement provides little insight except for the simplest of indeterminate problems such as parallel support rods with different properties or geometry, and fixed end conditions. An interesting attempt was made by Cane [19] to correlate grain boundary cavitations with physical damage. In this work, a damage parameter, A , the fraction of grain boundaries showing cavitations via microscopic inspection of acetate impressions, was substitute for w in the Kachanov equations. This allowed a direct prediction of remaining life. Unfortunately, later evaluation revealed too much scatter in the predictions for the method to be of practical use [20]. Kachanov equations will probably find their greatest use in combination with the finite element method in tackling complex multi-load path components. Significant work has already been done in this area. Hayhurst and Leckie [21] have derived equations extending the Kachanov method to multi-axial stress states:

$$\dot{w} = \frac{G[k\sigma_p + (1-k)\sigma_e]^m}{(1+p)(1-w)^p} \tag{10}$$

$$\dot{\epsilon}_{ij} = \left(\frac{3}{2}\right) B \sigma_e^{n-1} \frac{\sigma_{ij}}{(1-w)^n} \quad (11)$$

where G , p and m are creep constants determined as in the uniaxial case, σ_p and σ_e are the maximum principal and effective stresses, and k is a material parameter that must be determined from creep tests under at least two different stress states. This type of analysis utilizing the finite element method is relative new in the literature and has had very limited application in industry primarily due to the high cost of obtaining the required creep rupture data, the high costs in terms of computer time and the lack of verification research and analysis work to develop of cavity growth[21]. The traditional approaches described so far utilize a few standards parameters such as secondary creep rate ϵ_s , the rupture life t_r and the creep ductility ϵ_f neglecting the information available from the primary and tertiary creep stages. The justification used being that most materials stay in the secondary creep stage for a substantial portion of their life .However, with long times the tertiary creep becomes dominant which is not considered by these approaches. Therefore, the creep curve fitting methods covers those shortcomings. For instance, the theta projection method is an empirical procedure for resending strain and time trajectories. The theta projection was introduced by Brown et al. [22, 23] for extrapolating short term creep data to predict rupture time under isostress and isothermal conditions.

$$\epsilon^c = \theta_1(1 - e^{-\theta_2 t}) + \theta_3(1 - e^{-\theta_4 t}) \quad (12)$$

where ϵ^c is the creep strain, t is the time , and the terms, θ_{1-4} are experimentally determined constants. The equation models the primary and tertiary stages of creep, and implies that any constant secondary creep region is an inflection on the curve where the effects of strain hardening and strain softening processes are equal. Four θ parameters could be determined by using Eq. (12); therefore, 16 parameters are required to predict strain and time trajectories within the set of stress and temperature range [24, 25]. If rupture strain is constant, then an additional parameter is required for isothermal condition. On the other hand, the continuum damage mechanics concept requires at least 8 to 10 parameters depending on the number of damage mechanisms needed to be quantified in order to predict an accurate lifetime. Clearly, such a vast increase in complexity can only be justified if there is a big improvement on accuracy or much wider engineering usage [24]. Another method which defines the rate at which strain accelerates as results of creep strain is the MPC OMEGA:

$$\frac{d \ln \epsilon}{d \epsilon} = m + p + c = \Omega_p \quad (13)$$

This methodology uses the term Ω_p to take into account the cross sectional (m), creep (p) and other micro structural damage occurring during creep .This method relates the life fraction consumed to Ω_p as shown below:

$$\frac{t_s}{t_t} = \frac{\epsilon t_s \Omega_p}{(\epsilon t_s \Omega_p + 1)} \quad (14)$$

and

$$\epsilon_s = \frac{\ln(1 + t \epsilon \Omega_p)}{\Omega_p} \quad (15)$$

$$\epsilon_{os} = \frac{\epsilon}{(t_s \Omega_p \epsilon + 1)} \quad (16)$$

The key advantage of this method is that an estimate of the current strain rate in service and Ω_p gives a direct calculation of the life fraction consumed, by exposing the material properties at the operating stress and temperature.

Once the small amount of strain is measured, the stress or temperature may be increased slightly to obtain a creep plot with sufficient curvature to allow determination of Ω_p . However, Dyson [24] argues that the Omega method violates the physics underpinning the basis of the Omega parameter methodology and cannot be used to assess lifetimes of thermally degrading materials.

2.1 Reference stress method according to Ref. [5]

For steady state loading, the reference stress can be approximately determined by:

$$\sigma_{ref} = P \frac{\sigma_y}{P_L} = \frac{P}{\ln(R_0 / R_i)} \tag{17}$$

where P is the component load, P_L is the plastic collapse load at the yield strength σ_y when the material behaviour is taken to be elastic perfectly plastic. This assumes that the yield surface and creep deformation surface are similar in shape. Since the ratio σ_y/P_L is dependent only on the geometry for a given pattern of loading, an arbitrary value of σ_y may be used to determine P_L . Also, Eq. (17) is based on the Tresca yield criterion where the collapse mechanism is dominated by the hoop stress. In a welded pipe under hoop stress domination, the R5 suggest a stress redistribution factor denoted as k . Eq. (17) is rewritten as:

$$\sigma_{ref} = P \frac{\sigma_y}{P_L} = \kappa \frac{P}{\ln(R_0 / R_i)} \tag{18}$$

where k varies due to the creep deformation properties of each to the PM, HAZ and WM under the constraint of compatibility of PM/HAZ or/and HAZ/WM. The uniaxial rupture time for the PM and HAZ were assessed using the BS PD6605 procedure and the following master equation was derived [26, 27]:

$$\ln(t_u^*) = \beta_0 + \beta_1 \log(\sigma) + \beta_2 \sigma + \beta_3 \sigma^2 + \beta_4 T + \beta_5 / T \tag{19}$$

where t_u^* the predicted rupture time in hours, T is the absolute temperature and σ is the stress in $N\ mm^{-2}$ and the parameters β_i are given at $565^\circ C$ (refer to Table 1). For PM $k=1$, $k=1.4$ for HAZ as for the WM $k=0.7$ [11].

The weld material 1CrMo is widely used as tubes for boilers and heat exchangers and as components for pressure vessels. The uniaxial creep rupture data of 1CrMo steel tubes was analyzed in [26]. The master rupture curve obtained is given in Eq. (20):

$$\log_{10} t_r = -C + \frac{\beta_1}{\tau} + \left(\frac{\beta_2}{\tau}\right)\sqrt{\sigma} + \left(\frac{\beta_3}{\tau}\right)(\sqrt{\sigma})^2 + \left(\frac{\beta_4}{\tau}\right)(\sqrt{\sigma})^3 \tag{20}$$

Table 1
 β_i are constants with the following values for the PM and HAZ [26]

β_0	-39.765870
β_1	-8.43513298
β_2	-0.00186616660
β_3	$-2.91037377 \times 10^{-5}$
β_4	0.00935613085
β_5	49662.4102

Table 2 β_i are constants with the following values for 1CrMo [26]

C	20
β_1	22.349564
β_2	-0.195449
β_3	0.002218
β_4	-0.000251

Table 3 β_i are constants with the following values for the Mild Steel [28]

C	123.09
β_1	10^{-14}
β_2	-10^{-11}
β_3	10^{-08}
β_4	-10^{-5}
β_5	0.0153
β_6	-2.63

where t is the time-to-rupture in *hours*, σ is the stress in MPa and τ is given as [26]:

$$\tau = (\delta + 273) / 1000 \quad (21)$$

where δ is the temperature in °C. The values for the constant β_i for 1CrMo at 565 °C are given in Table 2. Also, another type of weld material is used within this paper and it is chosen to be the mild steel. Mild steel is known as Carbon Manganese steel. It contain less than 0.10% Carbon in Iron .Also, it contains Manganese which improves the strength whilst retaining the ductility. Therefore, for Carbon Manganese data at 565 °C is extrapolated using a polynomial fitting curve and it is obtained as[28]:

$$\ln(t_r) = C + \beta_1 \sigma^6 + \beta_2 \sigma^5 + \beta_3 \sigma^4 + \beta_4 \sigma^3 + \beta_5 \sigma^2 + \beta_6 \sigma \quad (22)$$

The values for the constant β_i for Mild Steel at 565 °C are given in Table 3:

2.2 Australian Standards: Code base approach for design life time in creep range

AS1210-1997 is the ‘Pressure Vessel’ design code in Australia and is equivalent to the American code ASME-VIII Div 1. AS1210-1997 which sets out the minimum requirements for design, manufacture, testing, inspection, certification and dispatch of fired and unfired pressure vessels constructed in ferrous or non ferrous metals by welding, brazing, casting, forging, or cladding and lining. This standard is only applicable with design pressure not exceeding 21MPa. However, the verification within this paper such as for the thick tube, thin tube and the pressurized welded tube (see section 4-5) are beyond the application limit of AS1210-1997. Therefore, for such cases, it is recommended to apply AS 4041-2006 which sets out minimum requirements for the material, design, fabrication, testing, inspection, reports and pre-commissioning of piping subjected to internal and external pressure or both. From table 1.4 of AS 4041-2006, there is no service limit on design pressure for class 1, and 10 to 100% radiography is required on Class 1 pipe and since the verified pressure vessels within this paper are seamless, the class 1 selection for all the vessels will be appropriate. Clause 3.14.3 of AS4041-2006 gives the equations for calculating the wall thickness of a pipe subjected to internal pressure having a wall thickness less than $D_0/6$. For thick wall tube the equation is given as:

$$P = f \log_e \left(\frac{D + 2t}{D} \right) \tag{23}$$

where D is the inner diameter, f is the design tensile strength, t is the minimum calculated thickness, P is the internal pressure

For the thin wall tube the equation is given as:

$$t_f = \frac{pD_o}{2feMW + p} \tag{24}$$

where t_f is the minimum calculated thickness, M is the class design factor equal to 1, W is the weld joint reduction factor equal to 1, e is the weld joint factor equal to 1. From Eq. (24) the design tensile strength is calculated. From Table D2 of AS4041-2006 Eqs. (25-30) are obtained using a regression form analysis from which the time-to-rupture is calculated and compared in tables (6-10).Eq. (25) represents a linear regressing form as for Eq. (26) it represents a logarithmic regression form of each of the parent material and heat-affected-zone.

$$f = 77 - 0.0002t_r \tag{25}$$

$$f = 288.15 - 19.73 \ln(t_r) \tag{26}$$

Eq. (27) and (28) represents the linear and logarithmic regression form for the 1CrMo, as for the Mild steel Eq. (29) represents the linear regression form and Eq. (30) represents the logarithmic regression form.

$$f = (-9 \times 10^{-5})t_r + 42.3 \tag{27}$$

$$f = -14.72 + 204.09 \ln(t_r) \tag{28}$$

Regression form equations for Carbon Manganese [28]:

$$f = (-0.0004)t_r + 73.556 \tag{29}$$

$$f = -13.91 + 19.8 \ln(t_r) \tag{30}$$

2.3 ASME standard B31: Code base approach for design life time in creep range

The ASME B31 Code for Pressure Piping consists of a number of individually published sections, each section reflect the kinds of piping installations considered during its development, as follows:

B31.1 covers the power piping system typically found in electric power generating stations, in industrial and institutional plants, geothermal heating systems, and central and district heating and cooling systems. Analytical Methodology in the code is based on thin shell linear elastic beam theorem. The code is developed to be used as a piping system design tool. The code is used to “prescribe the minimum requirements for the design, materials, fabrication, erection, test and inspection of power and auxiliary service piping systems”. It should be noted that B31.1 is not convenient for the component working in the creep range and is beyond the scope of the high temperature life assessment.

B31.3 includes the process piping typically found in petroleum refineries, chemical, pharmaceutical, textile, paper, semiconductor, and cryogenic plants, and related processing plants and terminals. In 2004, the ASME B31.3 added the weld joint factor strength reduction. This applies at temperature above 510 °C , and is based on consideration of the effects of creep. The weld reduction factor is applicable to the circumferential weld joints to evaluate the stresses due to the sustained loads denoted as S_L . Weld Reduction factor was added in the code because weldment creep rupture strength has been determined to be lower than base metal creep rupture in some circumstances [29]. The designer may determine the weld joint strength reduction factor for the specified weldment based on creep rupture test data. However, a simplified factor was provided for use by the designer in the absence of more applicable data. Because it is impractical to establish factors for specific materials, a general factor was used. The factor varies linearly from 1 at 510 °C to 0.5 at 810 °C .The designer can use other factors, based on creep tests.

The tests should be full thickness cross-weld specimens with test durations of at least 1000 hours. Full thickness tests are required unless the designer otherwise considers effects such as redistribution across the weld. The factor is applied to the allowable stress used when calculating the required thickness for internal pressure and when evaluating longitudinal stresses due to sustained loads. However, a limitation is imposed in B31.3 such as a reduction of short term allowable stress based on long term creep strength is not appropriate. Parent metal and cross-weld creep rupture data has been used to develop weld joint strength reduction factors provided in ASME section II, subsection NH. Factors for 100,000 hour durations were used in this paper. For the PM and HAZ a reduction factor of 1 was suggested (assuming 100% radiography), as for the WM a reduction factor of 0.8 is imposed. In [30], a detailed explanation is given on the evaluation of the weld reduction factor to express the rupture behavior in function of stress to rupture where the stress reduction factor is defined as:

$$R_{\sigma} = \frac{\sigma_w}{\sigma_p} \quad (31)$$

where σ_w is the rupture stress of the weld and σ_p is the rupture stress of the parent material consequently (refer to section 4). The code approach considered the hoop stress as the dominant, due to pressure throughout the wall thickness calculation:

$$S = \frac{1}{2EW} \left(\frac{PD}{t} - 2PY \right) \quad (32)$$

where S is the allowable stress, P is the internal design pressure, D is outside pipe diameter, E is quality factor equal to 1, W is weld joint reduction factor equal to 0.5, $PM=1$, $HAZ=0.8$, Y is coefficient (function of material and temperature equal to 0.7 at 565 °C), t is wall pipe thickness. Here, the hoop stress is calculated from the mean diameter formula:

$$S_{H,MD} = P \left(\frac{D_0 - t_n}{2} \right) / t_n \quad (33)$$

where t_n is the nominal wall thickness. However, the above aforementioned models ignore the effect of any plasticity on the life of the component. Zarrabi and Jelwan [5, 6] have previously developed a practical paradigm for predicting the lives of components subjected to elastic-plastic-creep deformation. This paper concentrates on creep and plasticity damages under non-cyclic loading. The total damage (D) due to plasticity (D_p) and creep (D_c) may then be represented by:

$$D = f(D_p, D_c) \quad (34)$$

Currently there is no generally accepted expression for the damage function $f(D_p, D_c)$ and failure models that combine plasticity and creep. For a properly designed mechanical component, as mentioned above, plastic damage is concentrated in the stress-concentration regions and its extent is limited. So in some cases, the analyst may consider the creep damage only. The content of this paper will describe a relatively accurate and practical model for predicting the life of a component subjected to elastic-plastic-creep deformation the details of which are described in Section 4 and 5.

3 STRAIN ENERGY DENSITY MODEL

The proposed paradigm allows the material to undergo an elastic-plastic-creep deformation but it postulates that the dominant damage mechanism is creep and at the point of failure the component fails by excessive creep deformation and/or creep rupture. This allows limited plastic deformation at the stress-concentration regions, which as mentioned above has practical significance, as the plastic deformation in the properly designed components is normally limited to the stress-concentration regions. Consider a component that is subjected to several loads. These loads are

increased in their respective magnitudes from zero to their operational levels over relatively short period of time so that it can be assumed that at time $t=0$ they instantly cause elastic deformation only in the regions where the corresponding equivalent stresses are below the yield strength and plastic deformation in the regions where the equivalent stresses are above the yield strength. Having reached their respective operational levels, the loads are taken to be constant causing creep damage/deformation until the point of failure. It is also assumed that the material temperature (T) is uniform and constant so that there is basically no fatigue damage. In the following, the superscript e refers to elastic; p refers to plastic and c refers to creep. At time t the rate of the total internal energy density (i.e., the rate of the total internal energy per unit of volume), $d\dot{W}$ may be expressed in terms of stress (σ_{ij}) and strain rate $\dot{\epsilon}_{ij}^k$ components as:

$$d\dot{W} = \sigma_{ij}(\dot{\epsilon}_{ij}^e + \dot{\epsilon}_{ij}^p + \dot{\epsilon}_{ij}^c) + \dot{W}_t \tag{35}$$

where \dot{W}_t is the rate of the internal (thermal) energy in the absence of stress at a point in the material. The total internal energy density at any point can be calculated by integrating Eq. (13) with respect to time:

$$W = \left\{ \iiint [\sigma_{ij}(\dot{\epsilon}_{ij}^e + \dot{\epsilon}_{ij}^p + \dot{\epsilon}_{ij}^c)] dt + \iint \dot{W}_t dt \right\} \tag{36}$$

Note that the second term in Eq.(35), i.e., $w_t = \iint \dot{W}_t dt$ is the input thermal energy density and it accounts for microstructural damages in the absence of stress. It may be calculated analytically for simple cases or numerically using the finite element method (FEM) for more complex cases. Note also that at the normal operational stress levels, the microstructural damages are also and indirectly accounted for by the pertinent material parameters. Therefore, one may postulate that at the normal operation where stresses are significant, then the first term (i.e., the strain energy density) in Eq. (36) is dominant and responsible for the damage in the material. On the other hand, as material is subjected to heat in absence of mechanical loading and constraints, the stresses are reduced and approach zero. This would cause W_t to be dominant and responsible for the damage. Previous investigations [31, 32] indicates that this postulation is valid. To obtain W using Eq. (12) then one needs first to compute the stresses and strains as functions of time up to the rupture time. For simple cases, this may be achieved analytically and for more complex cases a numerical method such as FEM may be employed. In determining the stress and strain fields as functions of time, the creep constitutive relationships up to the point of rupture including any tertiary region must be used, i.e., the model requires the inclusion of the creep tertiary response in the constitutive equation, which is normally obtained from uniaxial creep tests. If the tertiary creep response from uniaxial creep tests is not available, one can include the effects of the tertiary creep in the constitutive equation by suddenly increasing the creep strains at the uniaxial time-to-rupture (see Section 4 below). These data are part of the essential ingredients of any analysis involving creep deformation and normally obtained from the uniaxial creep tests. If no direct material data are available, published generic data may be utilised, with appropriate sensitivity analyses to cover the uncertainties. Note that in a creep finite element analysis, small time increments within the tertiary region and near the component rupture time are usually required but almost any finite element program with creep analysis capability that uses an inherent time integration algorithm may be used for this task - see, for example, Zarrabi and Hosseini-Toudeshky [33, 34]. In FEM, however, there will be a time at which a solution might not be converged for even very small time increments indicating the creep failure point of the component has been reached. Therefore, the model proposes that the computed W versus t graph be monitored. Referring to this graph, the proposed model characterizes the component failure when $\frac{dW}{dt} \rightarrow \infty$ or $\frac{dt}{dW} \rightarrow \infty$; see also Section 4.

4 STUDY CASE

Brown et al. [35] conducted an elastic-plastic-creep testing on a closed-ended thick tube with a central circumferential weld Fig.1. They carried out the tests at 565°C and experimentally determined the rupture time of the Mild steel weld as 14,691 hours and 18,774 hours when the vessel was welded with 1CrMo.

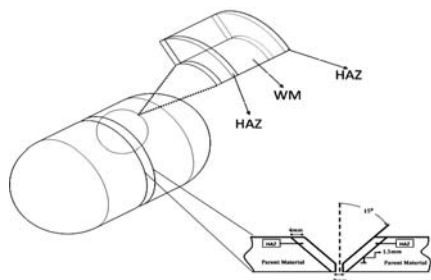


Fig. 1
Schematic Configuration of the Model and geometry of the HAZ.

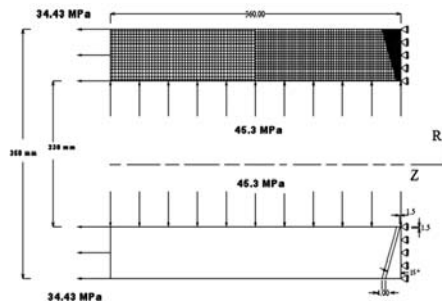


Fig. 2
Finite Element Model.

Table 4
Mechanical tensile properties [28]

At 565 °C	$E \times 10^6$ MPa	ν	σ_y MPa	ϵ_y $\times 10^{-4}$	σ_{vrs} MPa	ϵ_{vrs} $\times 10^{-2}$
0.5%Cr,0.5%Mo,0.25%V	0.1542	0.3	109.5	7.1	143	2.5
Mild Steel	154200	0.3	77	4.993	184	2.08
1CrMo	143000	0.3	92.875	6.494735	229.35	6.75

Table 5
Uniaxial creep data [35]

Creep properties	n	B
Parent material	8.831	8.12831×10^{-19}
Heat-Affected-Zone	6.267	1.34896×10^{-14}
Welding material (Mild Steel)	7.0004	6.77419×10^{-11}
Welding material (1CrMo)	8.4232	4.25598×10^{-14}

The tube was subjected to uniform internal pressure of 45.3 MPa which made this tube a suitable candidate for gauging the accuracy of the proposed model. The tube parent material (PM) was 0.5%Cr0.5%Mo0.25%V steel. The mechanical tensile properties of these materials at the test temperature of 565°C are shown in Table 4 [28]. The finite element model included the uniform end traction of 34.43 MPa to simulate the end loading due to internal pressure. The tube had an internal diameter of 230.00 mm and an external diameter of 350.00 mm and it was 720 mm long but because of symmetry half of its length (360 mm) was modeled for finite element analysis, (see Fig. 2).

Three thousand two hundred and eighty six 8-node axisymmetric elements were used to model the tube with 560 elements used to model the weld and 185 elements used to model HAZ. Element sizes in PM varied from 2 mm to 5 mm, and it was 0.75 mm in HAZ and 1 mm in the weld. The creep constitutive equations of each material were represented by:

$$\dot{\epsilon}^c = B\sigma^n \quad \text{if } t \leq t_r \quad (37)$$

$$\dot{\epsilon}^c = mB\sigma^n \quad \text{if } t \geq t_r \quad (38)$$

where B was the creep stress coefficient, n was the Norton stress index, t_r as the uniaxial time-to-rupture and the factor $m \geq 5$ was a constant. The values of B and n are listed in table 5 and they were average values obtained from uniaxial creep data reported graphically by Brown et al. [35]. These values when used in Equations (37) and (38) with stress in MPa gave creep strain rate in unit of mm/mm/hour. To describe the tertiary creep stage, the factor $m=5$ is included to represent a relative sudden increase in strain rate as the time-to-rupture is approached. It is worth noting that the actual value of m is somewhat arbitrary and the authors assumed that choosing $m=5$ is sufficient to impose a sudden increase in the creep strain rate when $t \geq t_r$ at a critically loaded point in the material to indicate the tertiary damage. ANSYS code [36] was used for the finite element analysis with a FORTRAN code developed by authors to link the creep constitutive equations defined by Eqs. (37) and (38) to ANSYS code. The uniaxial creep rupture data [35] was defined by Eq. (39) for PM, Eq. (40) for HAZ and Eq. (40) for the Mild Steel weld:

$$\sigma_r = -37.66 \log(t_r) + 299.84 \tag{39}$$

$$\sigma_r = -49.9 \log(t_r) + 386.94 \tag{40}$$

$$\sigma_r = -21.64 \log(t_r) + 144.58 \tag{41}$$

5 RESULTS AND DISCUSSION

5.1 Application to mild steel

The total strain energy density being a measure of plastic-creep damage was highest at the inner surface of the tube and Figs. 3 and 4 show the distributions of the total strain energy densities at the inner surface of the tube at $t=0$ hour and near the rupture time. Figs. 5 and 6 shows the distributions of stresses at the inner surface of the tube at $t=0$ hour and near the rupture time respectively. Referring to Fig. 3, it is apparent that initially the total strain energy densities were higher in WM and part of the HAZ than those in the parent material. Also, at $t=0$ hour the equivalent stress in PM and part of HAZ at the inner surface of the tube had just reached the yield strength indicating plastic deformation in these regions Fig. 5. With the passage of time and due to creep and further plastic deformation, the total strain energy density Fig. 4 were transferred from WM to HAZ causing further plastic and creep deformation in HAZ. This resulted in the highest total strain energy density (damage) accumulating at the inner surface and in HAZ causing eventual failure of the tube. The predicted failure location, correlated well with the HAZ cracking experimentally observed by Brown et al. [35].

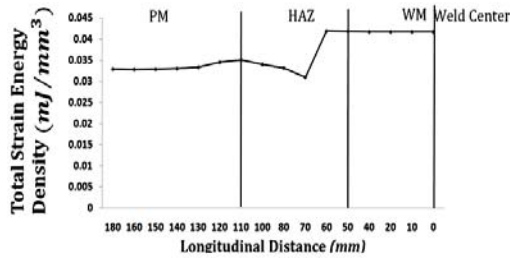


Fig. 3 Total strain energy density distributions at the inner surface of the tube at $t=0$ hour.

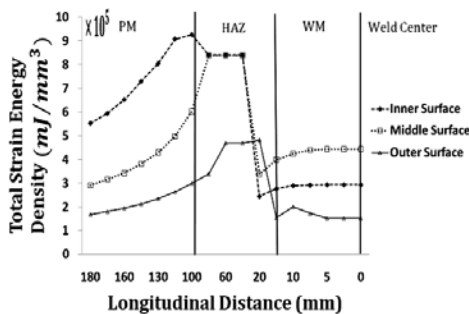


Fig. 4 Total strain energy density distributions at the inner, middle and outer surface of the tube at $t_r=13,524$ hours.

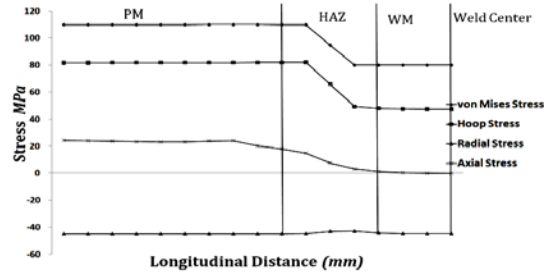


Fig. 5
Stress distributions at the inner surface of the tube at $t=0$ hour.

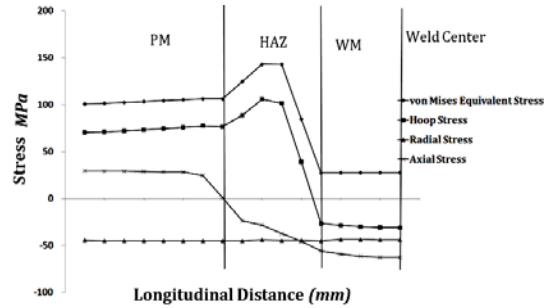


Fig. 6
Stress distributions at the inner surface of the tube at $t_r=13,524$ hours.

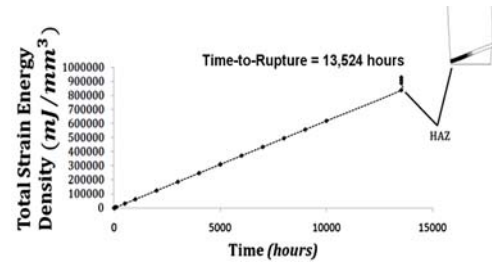


Fig. 7
Variation of the maximum strain energy density occurred at point A with time.

Table 6

Life of the PM predicted by various models. Note: Negative errors indicate non-conservative life prediction

Method	Stress (MPa)	Life Predicted (hours)	Error (%)	
Experimental	--	14.691	--	
Proposed Model (E.P.C.)	--	13.524	8	
Proposed Model (E.C.)	--	13.798	6	
Reference Stress (Eq. (5))	124	47.489	-223	
R5	Eq. (37)	108	124.165	-745
	Eq. (19)	108	15.222	-4
	Eq. (25)	108	-155.000	--
	Eq. (26)	108	9.235	37
A.S	Eq. (37)	108	124.165	-745
	Eq. (19)	108	15.222	-4
	Eq. (25)	108	-155.00	--
	Eq. (26)	108	9.235	37
ASME B31.3	Eq. (37) Eq. (32)	101	190.490	--
	Eq. (37) Eq. (33)	110	109.873	--
	Eq. (19) Eq. (32)	101	20.858	-42
	Eq. (19) Eq. (33)	110	15.468	-5
	Eq. (25) Eq. (32)	101	-120.000	--
	Eq. (25) Eq. (33)	110	-165.000	--
	Eq. (26) Eq. (32)	101	13.168	10
	Eq. (26) Eq. (33)	110	8.345	43

It is worth noting that stresses followed the same pattern as the total strain energy densities Figs. 4-6. The variation of the maximum total strain energy density with time is depicted in Fig. 7. Using the data shown in Fig. 7 and the proposed model the life of the tube is predicted as 13,524 hours, (see Table 3).By applying the minimum required thickness formula from ASME VIII-Div. 2 the allowable stress is calculated as 107.93 MPa. From Annex 3.A of ASME VII-Div.2 table 5A, part D, the allowable stress value for 0.5Cr-0.5Mo-0.25V was obtained as 17.93 MPa as for the weld allowable stress was 39 MPa. By referring to table 10-100 from appendix 10 of ASME VIII, Div.2 the minimum allowable stress for parent material is given. Hence, the parent material life is calculated as 125,003 hours, as for the weld the predicted life is 20,411 hours. The weldment strength reduction factor is calculated as 2.19 (using Eq. 31). Table 3 shows the life variation of the tube for each of the calculated weld reduction factor. Table 3 also includes the life of the tube estimated according to R5 [11, 12], ASME code B31.3 and the Australian Standard for comparison.

Table 7
Life of the HAZ predicted by various models. Note: Negative errors indicate non-conservative life prediction

Method	Stress (MPa)	Life Predicted (hours)	Error (%)	
Experimental	--	14.691	--	
Proposed Model (E.P.C.)	--	13.524	8	
Proposed Model (E.C.)	--	13.798	6	
Reference Stress (Eq. (5))	124	185.925	--	
R5	Eq. (38)	151	53.488	
	Eq. (19)	151	3.018	
	Eq. (25)	151	37.000	
	Eq. (26)	151	1.045	
A.S	Eq. (38)	108	124.165	
	Eq. (19)	108	15.222	
	Eq. (25)	108	-155.00	
	Eq. (26)	108	9.235	
ASME B31.3	Eq. (38)	126	169.535	
	Eq. (33)	110	354.732	
	Eq. (19)	Eq. (32) 126	7.506	49
		Eq. (33) 110	15.468	-5
	Eq. (25)	Eq. (32) 126	245.000	--
		Eq. (33) 110	-165.000	-
	Eq. (26)	Eq. (32) 126	3.709	75
		Eq. (33) 110	8.345	43

Table 8
Life of the WM predicted by various models. Note: Negative errors indicate non-conservative life prediction

Method	Stress (MPa)	Life Predicted (hours)	Error (%)	
Experimental	--	14.691	--	
Proposed Model (E.P.C.)	--	13.524	8	
Proposed Model (E.C.)	--	13.798	6	
Reference Stress (Eq. (5))	124	9	100	
R5	Eq. (39)	76	1.476	
	Eq. (22)	76	1.309	
	Eq. (30)	76	-6.110	
	Eq. (31)	76	97	
A.S	Eq. (39)	108	325	
	Eq. (22)	108	465	
	Eq. (30)	108	-8.6110	
	Eq. (31)	108	472	
ASME B31.3	Eq. (39)	Eq. (32) 201	405	97
		Eq. (33) 110	40	100
	Eq. (22)	Eq. (32) 201	--	--
		Eq. (33) 110	1.023	93
	Eq. (30)	Eq. (32) 201	-318.610	--
		Eq. (33) 110	-91.110	--
	Eq. (31)	Eq. (32) 201	51.743	-252
		Eq. (33) 110	522	96

5.2 Application to 1CrMo

The uniaxial creep rupture data [35] for 1CrMo was defined by Eq. (42)

$$\sigma_r = -37.96 \log(t_r) + 306.55 \quad (42)$$

Fig. 8 shows the variation of the stresses for elastic-creep analysis at the inner surface of the vessel at time equal 0 hour and at time-to-rupture respectively. Fig. 8 shows that at time=0 hour the equivalent stress was higher than the yield stress by 30%, which makes from the vessel a good candidate to analysis the impact of plasticity on the vessel deformation. Fig. 9 shows the variation of the von Mises stress, hoop stress and axial stress from the inner surface to the outer surface at time=0 hour for an elastic-plastic-creep analysis. Fig. 9 shows the computed equivalent stress in the parent metal were higher than those in the weld, indicating that the plastic deformation occurs within the PM and part of HAZ at the inner surface and it decreases gradually throughout the wall thickness of the tube till the steady state stress occurs at the outer surface. After the passage of time, the equivalent stress were transformed from the PM and they were concentrated in the heat affected zone (refer to Fig. 10).

Fig. 11 and 12 shows the distributions of the hoop and von Mises equivalent stresses for HAZ computed using an elastic-creep analysis respectively. As might be expected, Fig. 11 and 12 demonstrate the redistribution of initial elastic stresses due to creep. For comparison, Fig. 13 shows the distributions of the von Mises equivalent stresses computed using an elastic-plastic-creep analysis respectively. Here, the initial elastic stresses are redistributed by the initial plastic deformation. As a consequence, there is no significant stress redistribution due to the follow-up creep deformation and the variations of stresses with time is minimised. Referring to Fig. 13 it is apparent that no skeletal stress could accurately be defined. For the elastic-creep Fig. 11 and 12 show that while the hoop stress at the inner surface was lower than the hoop stress at the outer surface, the reverse was true for the von Mises equivalent stress. This was due to high negative (compressive) radial stress at the inner surface and approximately zeros radial stress at the outer surface that would affect the von Mises stress distribution for each of the PM, HAZ and WM (refer to Fig. 14,15 and 16). Comparing Fig.15 and 16 the distribution of the radial stress varies with a very abrupt change occurring across the heat-affected zone (Fig. 12). This arises due to the differences in the creep characteristics of the different part of the tube (PM, HAZ, and WM); the weld metal having a high ductility resistant in comparison with that for the parent metal.

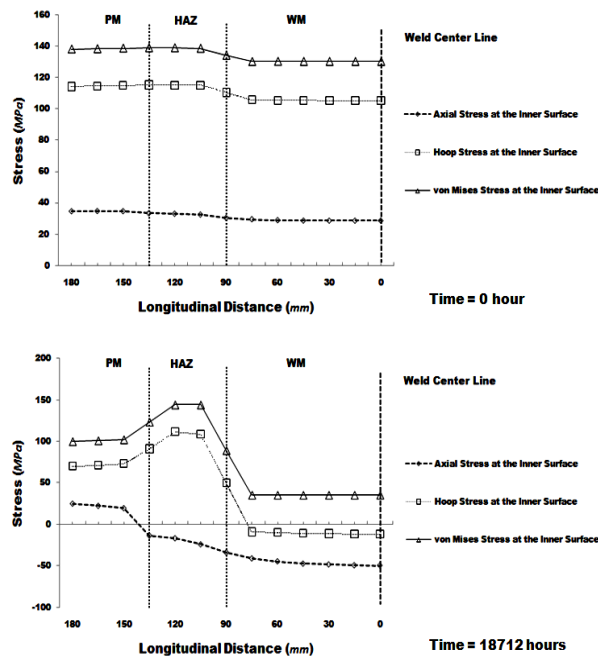


Fig. 8

Variation of von Mises equivalent stress, hoop stress and axial stress at the inner surface at time=0 hour and at time-to-rupture for elastic-creep analysis.

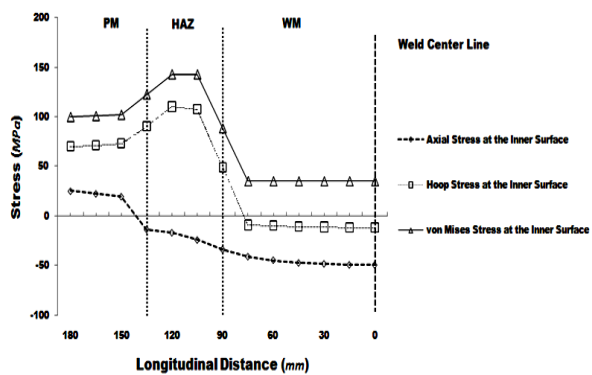
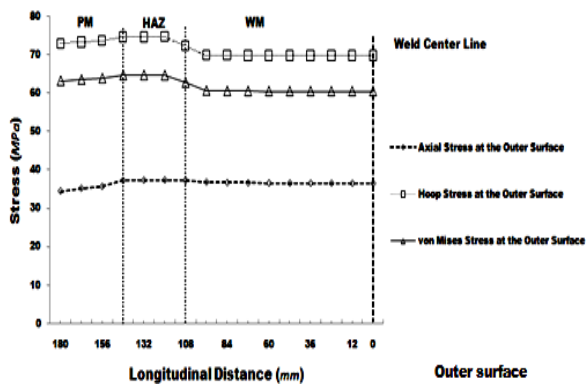
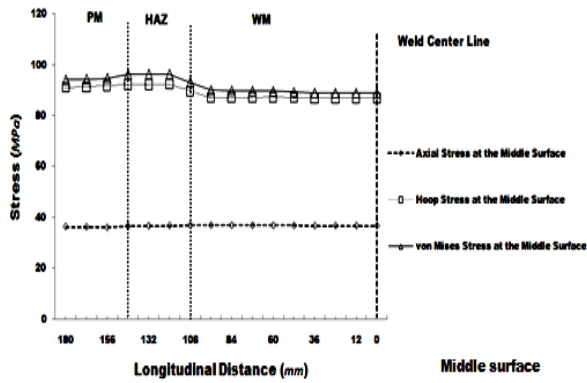
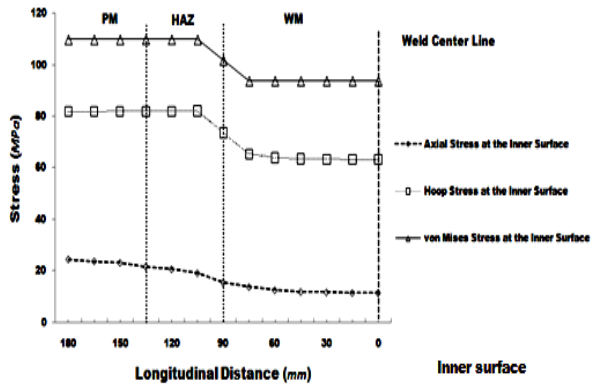


Fig. 9
Variation of von Mises equivalent stress, hoop stress and axial stress from the inner surface to the outer surface at time=0 hour for an elastic-plastic-creep analysis.

Fig. 10
Variation of von Mises equivalent stress, hoop stress and axial stress of the inner surface at time=18697 hours for an elastic-plastic-creep analysis.

Also, the difference in the material properties resulted in this severe stress redistribution from the weld metal into the heat-affected zone and the parent metal corresponds to a severe stress gradient observed in the heat-affected zone where Fig. 8 shows the severity of the hoop stress concentration in the HAZ which is growing throughout the wall thickness of the pipe, whereas little stress is conceded by the weld metal. The maximum strain energy density occurred at the inner surface the variation of which with time is depicted in Fig.17. Using the data shown in Fig. 7 and the proposed paradigm the life of the vessel is predicted as 18,691 hours, see also Table 9. Table 9 also includes the predicted lives of the vessel using the reference stress method and Robinson time fraction rule as well as the experimental life for comparison. The data in Table 9 show that while the proposed model accurately predicted the life of the vessel the other methods were non-conservative for this application. This might be expected as strictly, the reference stress method and Robinson time fraction rule are applicable to elastic-creep damages and not elastic-plastic-creep damages.

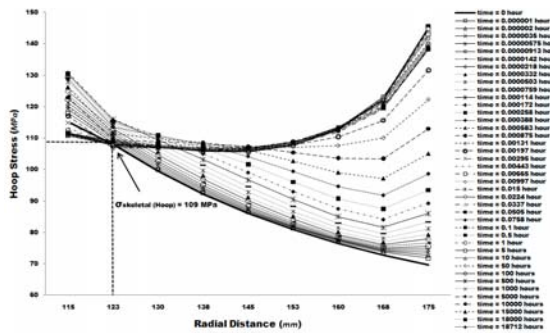


Fig. 11
Hoop stress versus radial distance at various time points computed using an elastic-creep analysis.

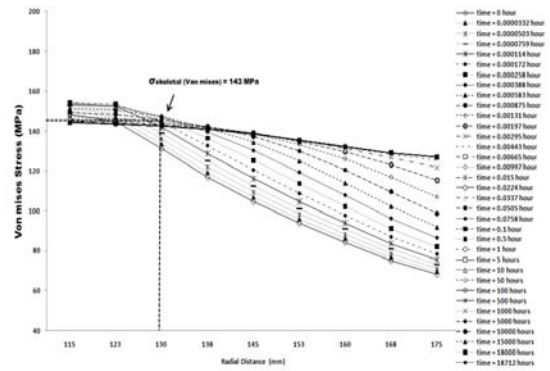


Fig. 12
von Mises equivalent stress versus radial distance at various time points computed using an elastic-creep analysis.

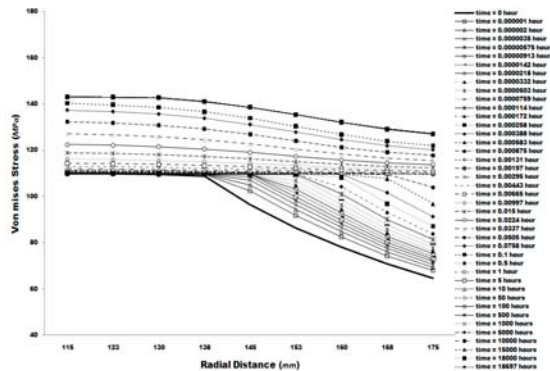


Fig. 13
von Mises equivalent stress versus radial distance at various time points computed using an elastic-plastic-creep analysis.

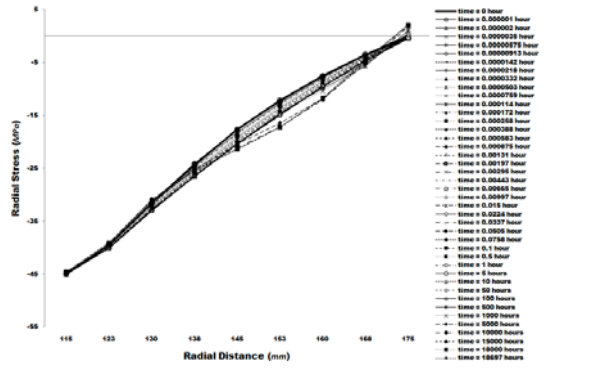


Fig. 14
Radial stress versus radial distance at various time points computed using an elastic-plastic-creep analysis (PM).

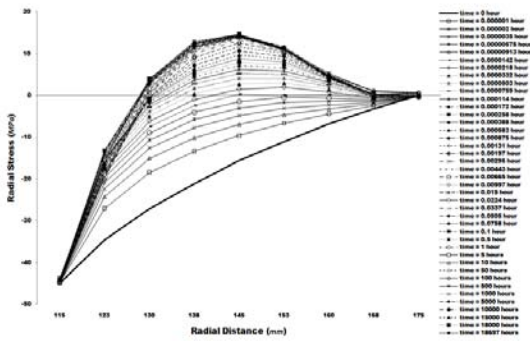


Fig. 15
Radial stress versus radial distance at various time points computed using an elastic-plastic-creep analysis (HAZ).

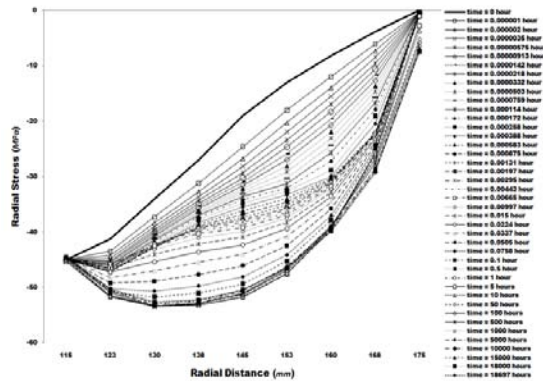


Fig. 16
Radial stress versus radial distance at various time points computed using an elastic-plastic-creep analysis (WM).

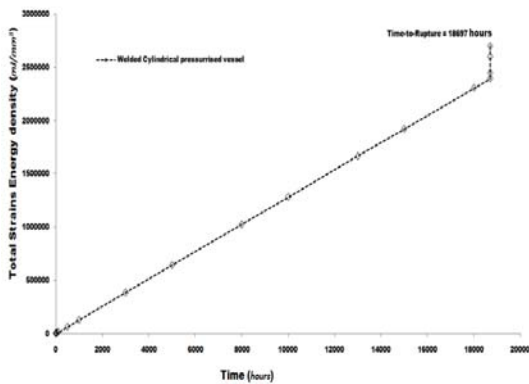


Fig. 17
Total strain energy density versus time at the inner surface of the vessel.

Table 9

Life of the WM predicted by various models. Note: Negative errors indicate non-conservative life prediction

Method	Stress (MPa)	Life Predicted (hours)	Error (%)	
Experimental	--	18.774	--	
Proposed Model (E.P.C.)	--	18.697	0.4	
Proposed Model (E.C.)	--	18.712	0.3	
Reference Stress (eq.5)	124	64.418	-243	
Robinson Rule Eqt.1	E.P.C	30.148	61	
	E.C	30.451	62	
Skeletal Stress (HAZ)	Hoop Stress	16.0016	-752	
	Von Mises Stress	20.346	-8	
	Eq. (40)	1184.100	--	
R5	Eq. (20)	48.994	-161	
	Eq. (26)	-374.444	--	
	Eq. (27)	9.981	47	
A.S	Eq. (40)	170.022	-806	
	Eq. (22)	15.703	16	
	Eq. (32)	603	97	
ASME	Eq. (40)	Eq. (33)	150.598	-702
B31.3	Eq. (22)	Eq. (32)	201	1.101
		Eq. (33)	110	14.776
			110	21

6 CONCLUSIONS

The problem associated for predicting the remaining life of welded tube still a complex subject for analyst. Many difficulties are imposed when designing the creep strength reduction factor for weldment, under a multiaxial stress/strain filed. Table 8 shows how difficult are to define the weld reduction factor either indirectly or by straight forward application to obtain the most appropriate factor. This may not be the only reason too, as other factors are incorporated too, such as the approximation for the weld material properties and the lack of experimental data. Most designs are based on 100,000 hours properties. Since it is economically and practically not feasible to conduct 100,000 hours stress rupture tests, some means must be found to predict long-time rupture strengths from short time data .Two such methods are parametric evaluations and straight line extrapolation. Parametric evaluations are mathematical relations in which rupture life is a function of temperature and stress. Since the parameter value is a function of stress, a smooth curve should result from a log stress versus parameter plot (refer to Eq. 25 and 30). Such a curve can be extrapolated to predict stress rupture behavior at times exceeding actual test times. The major criticism of the straight line/or linear extrapolation method is that structural changes may occur within the material and change the slope of the log stress versus log rupture time curve. Also, the principal limitations of parametric analyses of creep rupture data that the AS1210 assessment code life suggest can be criticized by the insufficient raw data to generate adequate stress calculations for the Manson-Haferd parameter, problems with compacted scale plotting, the tendency to extrapolate the extrapolation and difficulties in getting a suitable fit for the parametric relationship involved with the provided data. This paper identify a need to provide a serious consideration for an appropriate weld strength factor which would be applied to the vessel and to improve the criteria related to design against creep and the prevention of failure. It is shown that the elastic-plastic-creep damage model based on the exhaustion of the strain energy density at critically loaded regions in the material can accurately be applied to welded joints. For the welded tube considered in this paper the proposed model predicted the life of the tube conservatively with an error less than 10%.

However, it is worth noting that creep lives may be sensitive to some material parameters such as n (creep stress exponent) and one needs to perform appropriate sensitivity analysis before making the final conclusion. For instance, Fig. 19 shows how the Norton creep stress coefficient can affect the results. B varied from $4.043181e-14$ to $4.468779e-14$ ($\pm 5\%$) based on the creep material data extracted from Brown at al. [35]. This results in a variation of 16,104 to 15,907 hours (or 14.22% to 15.27%). It seems that the 1CrMo weld material properties for Norton coefficient does not greatly affect the time-to-rupture of the specimen. Conducting the sensitivity analysis on the stress index (Fig. 18), which varied from 8.36095 to 9.24105 ($\pm 5\%$) based on the creep material data. This results in a variation of 19,154 to 13,146 hours (or -2.03% to -29.98%). Results show that the Norton stress index can greatly affect the time-to-rupture of the 1CrMo weld material. The summarized values are compiled in table 10. The proposed model is based on multiaxial stress and strain fields and as such takes into accounts the internal forces and

deformation in the material. The proposed model is relatively simple to employ in practice due to the scalar nature of the strain energy density. The model takes into account creep and plasticity, and research is currently in progress to include the fatigue damage. Also, as Wilshire and Scharning [37] have pointed out, creep lives are governed by accumulation of strains and therefore the methods that take into account stress values only might not results in valid predictions ,which is the case of the ASME B31.3 ,R5 and the Australian Standard.

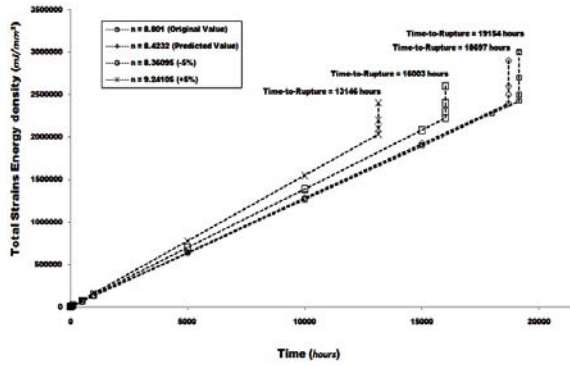


Fig. 18
Sensitivity analysis of the predicted value “n” for 1CrMo WM at 45.3 MPa.

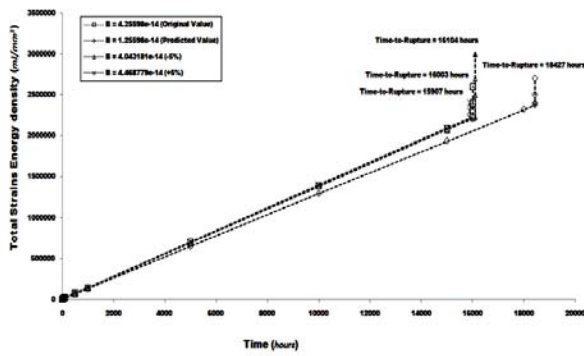


Fig. 19
Sensitivity analysis of the predicted value “B” for 1CrMo WM at 45.3 MPa.

Table 10
Summary for the variation of “n” & “B” for 1CrMo WM at 45.3 MPa

1CrMo WM	Experimental Life (hours)	Predicted Life (hours)	% Δ_{Lj}	n_p	n_o	% Δ_n	$B_p \frac{1}{hour/MPa^n}$	$B_o \frac{1}{hour/MPa^n}$	% Δ_B
	18774	16003	14.76%		n=8.801			B=4.26E-14	
5%MIN of “n”	18774	19154	-2.03%	n=8.36095	n=8.801	-5.00%	B=4.26E-14	B=4.26E-14	0%
5%MAX of “n”	18774	13146	29.98%	n=9.24105	n=8.801	5.00%	B=4.26E-14	B=4.26E-14	0%
5%MIN of “B”	18774	16104	14.22%	n=8.801	n=8.801	0%	B=4.04E-14	B=4.26E-14	-5.00%
5%MAX of “B”	18774	15907	15.27%	n=8.801	n=8.801	0%	B=4.47E-14	B=4.26E-14	5.00%
SENSITIVITY ANALYSIS for “n”	18774	18697	0.41%	n=8.4232	n=8.801	-4.29%	B=4.26E-14	B=4.26E-14	0%
SENSITIVITY ANALYSIS for “B”	18774	18427	1.85%	n=8.801	n=8.801	0%	B=1.26E-14	B=4.26E-14	-70.49%

ACKNOWLEDGEMENTS

The Authors would like to thank Associate Professor Zarrabi for his helpful discussions, information and expert advice given in the area of creep analysis, as well as allowing us to conduct the analysis by using his pragmatic model in order to obtain certain insights into the life assessment prediction for pressure vessels subjected to elastic-plastic-creep deformations.

REFERENCES

- [1] Portevin A., CR Acad C.,1923, *Science* **176**: 507.
- [2] Sawada K., Kubo K., Abe F., 2001, Creep behavior and stability of MX precipitates at high temperature in 9Cr-0.5Mo-1.8W-VNb steel. *Materials Science and Engineering A* **319-321**: 784-787.
- [3] R5, 1995, *Assessment Procedure for the High Temperature Response of Structures*, Berkely Technology Center, Nuclear Electric plc, (Issue 2).
- [4] ASME S., III, *Rules for Construction of Nuclear Power Plant Components*, ASME,USA, 2009, Division 1, Sub-Section NH, Class 1 Components in Elevated Temperature Service.
- [5] Zarrabi K., J.J., Mamood T., 2010, A Mesoscopic damage model for predicting the plastic-creep life of welded joints subjected to quasi-static loading, *Proceedings of ASME IMECE, ASME 2010 International Mechanical Engineering, Congress and Exposition*, November 12-18, 2010, Vancouver, British Columbia, Canada, IMECE2010-37042.
- [6] Zarrabi K., J.J., 2010, Integrity assesment of notched bars subjected to elastic-plastic-creep damage employing multiaxial stress/strain fields, *International Journal of Materials Engineering and Technology* **3**(2): 173-187.
- [7] Robinson E.L., 1952, Effect of Temperature Variation on the Long-Time Rupture Strength of Steels, *ASME*, **74**: 777-780.
- [8] Viswanathan R., 1989, *Damage Mechanisms and Life Assessment of High Temperature Components*, ASM International, Metals Park, OH, 447.
- [9] Stigh U., 2006, Continuum Damage Mechanics and the Life-Fraction Rule, *ASME Journal of Applied Mechanics* **73**(4): 702-704.
- [10] Webster G.A., Holdsworth S.R., Loveday M.S., Nikbin K., Perrin I.J., Purper H., Skelton R.P., Spindler M.W, 2004, A code of practice for conducting notched bar creep tests and for interpreting the data, *Fatigue and Fracture of Engineering Materials and Structures* **27**(4): 319-342.
- [11] Spence J.T.B.A.J.,1983, *Stress Analysis for Creep*, Butterworths, London 119.
- [12] Zarrabi K., 1993, Estimation of boiler tube life in presence of corrosion and erosion processes, *International Journal of Pressure Vessels and Piping* **53**(2): 351-358.
- [13] A., S., 2003, Creep and high temperature failure, in: *Comprehensive Structural Integrity* **5**, Elsevier, Pergamon,UK.
- [14] Kachanov L.,1958, *Time of the Rupture Process Under Creep Conditions*, Izv. AN SSSR, Otd. Tekhn, Nauk.
- [15] N., R. Y., *Proceedings of XII IUTAM Congress*, Stamford, CN, edited by Hetenyi and Vincenti, Springer, 1969, 137.
- [16] Penny R.K., Marriott D.L., 1995, *Design for Creep*, Chapman and Hall,London, UK.
- [17] Cane B.J., Williams J.A., 1987, Remaining life prediction of high temperature materials, *International Materials Reviews* **32**: 241-264.
- [18] Shammass M.S., 1987, *Estimating the Remaining Life of Boiler Pressure Parts*, EPRI Final Report on RP2253-1,4, Electric Power Research Institute, Palo Alto, CA.
- [19] Cane, B.J., Shammass, M.S.,1984, *A Method for Remanent Life Estimation by Quantitative Assessment of Creep Cavitation on PLant*, Report TPRD/L/2645/N84, Central Electricity Generating Board, Leatherhead.
- [20] Eillis F.V., Henry J.F., Shammass M.S., 1989, *Remaining Life Estimation of Boiler Pressure Parts,4,Metallographic Models for Weld Heat Affected Zone*, EPRI Report CS-5588, Electric Power Research Institue, Palo, Alto,CA, USA.
- [21] Hayhurst D.R.L., F A.,1983, *Behaviour of materials at high temperatures*. Mechanical behaviour of materials - IV; *Proceedings of the Fourth International Conference*, Stockholm, Sweden;, 15-19 Aug, 1195-1211, UK.
- [22] Brown S.G.R., Evans R.W., Wilshire B., 1986, A comparison of extrapolation techniques for long-term creep strain and creep life prediction based on equations designed to represent creep curve shape, *International Journal of Pressure Vessels and Piping* **24**(3): 251-268.
- [23] Brown S.G.R., Evans R.W., Wilshire B., 1986, Creep strain and creep life prediction for the cast nickel-based superalloy IN-100, *Materials Science and Engineering* **84**: 147-156.
- [24] Dyson B., 2000, Use of CDM in Materials Modeling and Component Creep Life Prediction, *Journal of Pressure Vessel Technology* **122**(3): 281-296.
- [25] McLean M., Dyson B.F., 2000, Modeling the Effects of Damage and Microstructural Evolution on the Creep Behavior of Engineering Alloys, *Journal of Engineering Materials and Technology* **122**(3): 273-278.
- [26] Budden P.J., 1998, Analysis of the Type IV creep failures of three welded ferritic pressure vessels, *International Journal of Pressure Vessels and Piping* **75**(6): 509-519.

- [27] Abe F., W.B., Doi H., Hald J., Holdsworth S.R., Igarashi M., Kern T.-U., Kihara S., Kimura K., Kremser T., Lizundia A., Maile K., Masuyama F., Merckling G., Minami Y., Morris P.F., Muraki J.O. T., Sandstrom R., Schubert J., Schwass G., Spindler M., Tabuchi M., Yagi K., Yamada M., 2004, Creep Properties of Heat Resistant Steels and Superalloys, in: *Numerical Data and Functional Relationships in Science and Technology*, Group VIII: Advanced Materials and Technologies, Subvolume B, **2**, Springer-Verlag Berlin, Heidelberg, New York.
- [28] *High Temperature Design Data for Ferritic Pressure Vessel, 1983*, Mechanical Engineering Publications, Institution of Mechanical Engineers (Great Britain), Creep of Steels Working Party.
- [29] Charles B., 2009, *IV Process Piping: The Complete Guide to ASME B31.3*, Third Edition, ASME, USA.
- [30] Tu S.-T., Segle P., Gong J.-M., 1996, Strength design and life assessment of welded structures subjected to high temperature creep, *International Journal of Pressure Vessels and Piping* **66**(1-3): 171-186.
- [31] Zarrabi K., Ng L., 2008, A Novel and simple approach for predicting creep life based on tertiary creep behavior, *Journal of Pressure Vessel Technology* **130**(4): 041201.
- [32] Zarrabi K., N.L., 2007, An energy based paradigm for predicting creep life based on tertiary creep behavior, *The International Journal of Science and Technology -Scientia Iranica - Transactions on : Mechanical and Civil Engineering* **14**: 450-457.
- [33] Zarrabi K., H.-T.H., 1997, An innovative robust method for creep life assessments of components containing stress concentrators under primary plus secondary creep, in: *Proceedings of the International Joint Power Generation Conference and Exposition*, edited by A. Sanyal, A. Gupta and J. Veilleuxn, 2-5 November, EC-Vol.5, ASME, Denver, USA.
- [34] Zarrabi K., Hosseini-Toudeshky H., 1995, Creep life assessments of defect-free components under uniform load and temperature, *International Journal of Pressure Vessels and Piping* **62**(2): 195-200.
- [35] Brown R.J., B.J.C., Walters D.J., 1981, Creep Failure analysis of butt welded tubes, *Proceedings of the 1st International Conference on Creep and Fracture of Engineering Materials and Structures*, Swansea, Pineridge Press, 645-659.
- [36] ANSYS, ANSYS Release 12.0, ANSYS, Inc., MAY-2008, USA.
- [37] Wilshire B., Scharning P.J., 2008, Extrapolation of creep life data for 1Cr-0.5Mo steel, *International Journal of Pressure Vessels and Piping* **85**(10): 739-743.